Human body shadowing in cellular device-to-device communications: channel modeling using the shadowed fading model

Cotton, S. L. (2015). Human body shadowing in cellular device-to-device communications: channel modeling using the shadowed fading model. IEEE Journal on Selected Areas in Communications, 33(1), 111-119. DOI: 10.1109/JSAC.2014.2369613

Published in:
IEEE Journal on Selected Areas in Communications

Document Version:
Publisher's PDF, also known as Version of record

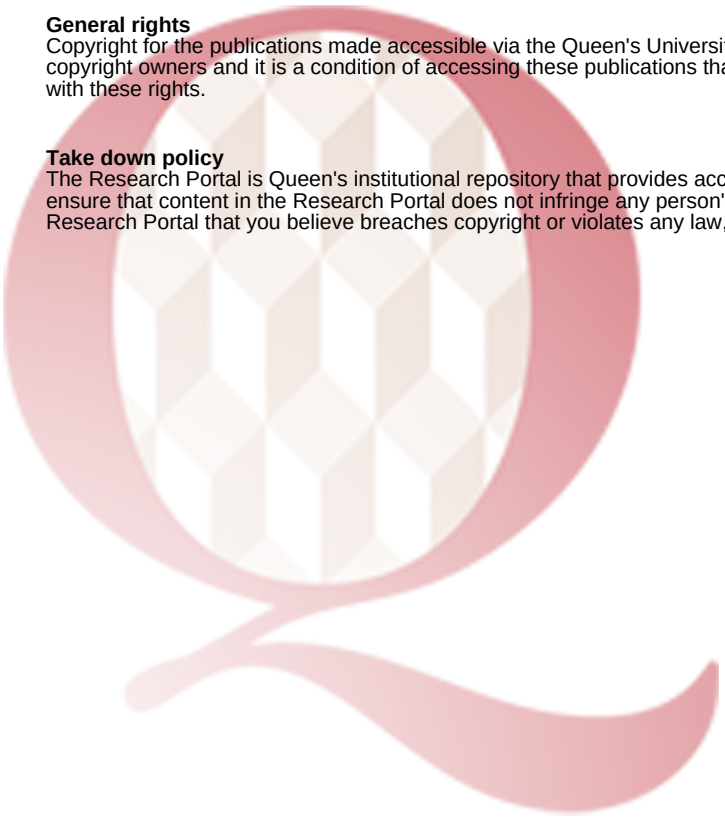

Human Body Shadowing in Cellular Device-to-Device Communications: Channel Modeling Using the Shadowed $\kappa - \mu$ Fading Model

Simon L. Cotton, *Senior Member, IEEE*

***Abstract*—Using device-to-device communications as an underlay for cellular communications will provide an exciting opportunity to increase network capacity as well as improving spectral efficiency. The unique geometry of device-to-device links, where user equipment is often held or carried at low elevation and in close proximity to the human body, will mean that they are particularly susceptible to shadowing events caused not only by the local environment but also by the user's body. In this paper, the shadowed $\kappa - \mu$ fading model is proposed, which is capable of characterizing shadowed fading in wireless communication channels. In this model, the statistics of the received signal are manifested by the clustering of multipath components. Within each of these clusters, a dominant signal component with arbitrary power may exist. The resultant dominant signal component, which is formed by the phasor addition of these leading contributions, is assumed to follow a Nakagami-m distribution. The probability density function, moments, and the moment-generating function are also derived. The new model is then applied to device-to-device links operating at 868 MHz in an outdoor urban environment. It was found that shadowing of the resultant dominant component can vary significantly depending upon the position of the user equipment relative to the body and the link geometry. Overall, the shadowed $\kappa - \mu$ fading model is shown to provide a good fit to the field data as well as providing a useful insight into the characteristics of the received signal.**

***Index Terms*—Device-to-device communications, shadowing, channel measurements, channel modeling, $\kappa - \mu$ distribution.**

I. Introduction

THE ever increasing demand for high data rate applications on the move has meant that cellular network and mobile hardware designers continue to vigorously push the boundaries on the maximum rate at which information can be transmitted over wireless communications channels. One method of supplementing cellular communications, which is currently gaining significant momentum through IMT-Advanced [1], is to use network users themselves as relays by employing device-to-device (D2D) communications [2]–[9]. In this device-to-device model, existing cellular infrastructure can be used to setup, control and manage short direct communications links between nearby cellular device users within an operator's network [2]. It has been proposed that the actual level of involvement of cellular operators may range from full control of D2D communications—where the cellular network has responsibility for control plane and data plane functions through to loosely controlled D2D communications—where operators perform access authentication only, thus allowing localized devices to setup and start D2D communications autonomously [3].

Loosely controlled D2D communications will most likely use technologies operating within the unlicensed Industrial Scientific and Medical (ISM) bands centered at 2.45 GHz and 5.8 GHz as most smart devices now come with wireless chipsets that will support at least one of these two frequencies. In this part of the spectrum, D2D users will have to compete with other wireless users, for example those using Bluetooth, Wi-Fi, ZigBee and other proprietary technologies to communicate. As highlighted in [10], another potential drawback of using established ad hoc networking protocols for D2D communications is that they may require direct user intervention to establish network connections, a feature which is likely to prove unpopular with end users. In contrast, fully controlled D2D communications will almost certainly use cellular frequencies, as the network operator will need to regulate all aspects of the D2D connection. One of the key advantages of using licensed cellular frequency allocations for D2D communications is that they can be effectively managed using current infrastructure to limit potential interference from other nearby users. An architecture for this was proposed in [2], where D2D communications were considered as an underlay for a Long Term Evolution (LTE) Advanced network. Using dedicated signaling for session setup and the automatic handover of network routed traffic to D2D links, it was shown that even for the worst case scenario of interference limited D2D communications an increase in the total throughput in a local cell area can be achieved.

Reducing interference in D2D communications will require judicious adaptive power control that not only aims to reduce interference with other cellular users, but also takes into account fading and User Equipment (UE) mobility. This will be essential to ensuring that D2D links can be practically maintained and assist with the decision as to whether a link should be abandoned and data rerouted through another UE or off-loaded to the base station (BS), or equivalently evolved NodeB (eNB) in the case of LTE. Optimal power control for D2D communications [1], [11]–[13] will therefore require an intricate knowledge of the channel between co-located D2D

Manuscript received May 20, 2013; revised November 15, 2013; accepted August 5, 2014. Date of publication November 11, 2014; date of current version January 30, 2015. This work was supported in part by the U.K. Royal Academy of Engineering, by the Engineering and Physical Research Council (EPSRC) under Grants EP/H044191/1 and EP/L026074/1, and by the Leverhulme Trust, U.K.

The author is with the Institute of Electronics, Communications and Information Technology, Queen's University Belfast, Belfast BT3 9DT, U.K. (e-mail: simon.cotton@qub.ac.uk).

Color versions of one or more of the figures in this paper are available online at http://ieeexplore.ieee.org.

Digital Object Identifier 10.1109/JSAC.2014.2369613

users. In conventional cellular communications the BS is fixed, typically elevated and often relatively free of local scattering. However in D2D channels, both the transmitter and receiver are in close proximity to the human body (e.g., in a pocket or held), often in motion and at relatively low elevation compared to base stations. Due to the nature of human behavior, D2D communications links will be subject to stochastic shadowing events caused by the user's body [14], [15] intersecting and shadowing the direct line of sight (LOS) signal path between UEs. Furthermore, as humans may spend a significant amount of time in populated environments, these links will also be heavily susceptible to shadowing and scattering caused by differing pedestrian densities as well as being affected by other obstacles such as vehicles, buildings and vegetation.

In this paper a novel, very general statistical model is proposed in which the resultant dominant component is subject to random shadowed fading. The utility of the new model for characterizing signal reception in D2D communications is then validated through field measurements. In this model clusters of multipath are assumed to have scattered waves with identical powers, alongside the presence of elective dominant signal components—a scenario which is identical to that observed in $\kappa-\mu$ fading [16]. The $\kappa-\mu$ distribution is an extremely versatile fading model which contains as special cases other important distributions such as the One-Sided Gaussian, Rice (Nakagami-n), Nakagami-m and Rayleigh distributions. While the model proposed here inherits all of this generality, the critical difference between this model and that of $\kappa-\mu$ fading is that the resultant dominant component, formed by phasor addition of the individual dominant components[1] is assumed to be random. In particular it is assumed that this resultant dominant component follows a Nakagami-m distribution. Hence the model proposed here is appropriately named as the shadowed $\kappa-\mu$ fading model.

The remainder of this paper is organized as follows. Section II presents a discussion of the main propagation phenomena likely to be associated with shadowed fading in D2D channels. The complex signal model proposed for shadowed $\kappa-\mu$ fading in wireless communications channels is introduced in Section III. Novel expressions for the probability density function (PDF), moments and moment generating function (MGF) of the shadowed $\kappa-\mu$ fading model are also derived in Section III. Section IV presents the measurement setup used for the experimental part of this study. In Section V, an empirical validation of the proposed model is provided using a range of experiments aimed at replicating the shadowing conditions likely to be encountered in outdoor D2D channels. Finally, Section VI finishes the paper with some concluding remarks.

II. Signal Reception in Shadowed D2D Communications Channels

In the closely related research area of body centric communications, where wireless devices are also used in close proximity to the human body, the impact of shadowing upon physical layer links is reasonably well established [15], [17], [18]. For example in a low multipath environment [15], it was observed that the link between a chest worn patch antenna operating at 2.45 GHz and an identical antenna placed on a non-conductive pole at the same elevation deteriorated by 50 dB when the user's body turned to obstruct the main LOS path at a separation distance of 1 m. Clearly, shadowing caused by the human body can have a considerable effect upon the communications channel. This will be particularly prevalent in D2D communications, where the UE is often held in the user's hand, operated close to the head and positioned next to the user's body (e.g., in a pocket). Therefore, to engineer not only robust power control mechanisms but also hardware such as antennas and transceiver circuitry and optimize protocols to be used in D2D communications, the impact of human body shadowing should be included in physical layer models used to describe signal reception.

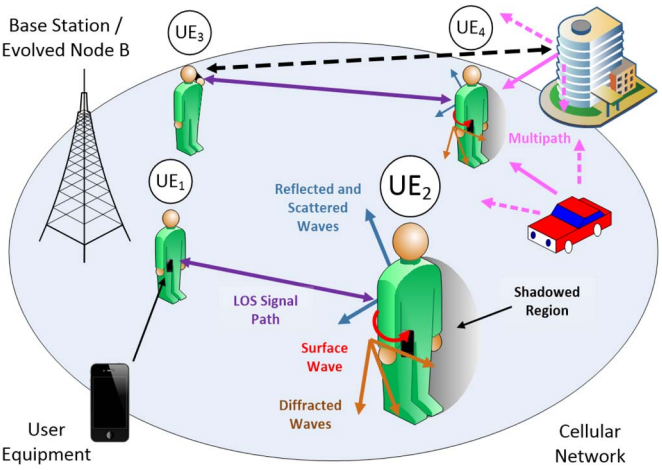

Fig. 1. Illustration of some the propagation mechanisms associated with shadowing in D2D communications.

For small changes in separation distance (i.e., on the order of wavelengths), Fig. 1 highlights the main propagation mechanisms encountered at ultra-high frequencies (from 300 MHz to 3 GHz) for device-to-device links in which the direct link between UEs is shadowed by the human body. If we initially consider the link between UE_1 and UE_2, here both devices are located in a pocket at the respective user's waist. As we can see the main LOS signal path from UE_1 to UE_2 is obscured by the second user's body. In this instance, if we initially ignore specular and multipath signal components generated by the local surroundings, the D2D link will be formed by a combination of reflected, diffracted, surface wave propagation [19] and non-homogeneous scattering from the second user's body in which none, one or more of these processes may instantaneously dominate the signal reception. To complicate matters further, due to physiological and biomechanical processes associated with the human body, the shadowing effect caused by the body will quite often be non-deterministic and must be treated as a random process.

As well as the propagation mechanisms discussed above, for the D2D link between UE_3 and UE_4 (Fig. 1), multipath generated by the local environment is also present which contributes to the overall signal reception. In this scenario, multipath clusters produced by the building and car will help mitigate

[1] It should be noted that the resultant dominant component here can be made up of leading signal components that arrive at the receiver by mechanisms other than just line of sight propagation.

the shadowing effect of the body. Within each of the clusters generated by the local surroundings, a signal component of arbitrary power may exist (e.g., caused by a specular reflection), which dominates over all of the scattered waves in that cluster. Given the proposed physical propagation phenomena described above, it seems plausible to assume that the received signal in shadowed D2D channels undergoes the same propagation mechanisms as that encountered in $\kappa-\mu$ fading [16] except in this instance the resultant dominant component, which is formed by the phasor addition of the leading signal components in the channel, is a random variable.

III. The Shadowed $\kappa-\mu$ Fading Model

Shadowed fading of the received signal has been observed in other areas of communications outside D2D communications such as land mobile satellite channels [20], [21]. Here shadowing of the LOS signal component is caused by complete or partial blockage of the LOS by environmental factors such as buildings, trees, hills and mountains etc., which in turn make the amplitude of the LOS component a random variable [20]. In [21], it is assumed that the short-term signal variation is due to Rice fading, in which the LOS component is shadowed and modeled by a lognormal distribution. This approach, however, can lead to statistical formulations which are difficult to manipulate analytically, and in the case of Loo's shadowed fading model [21] an expression which has no closed form. Following [20] the resultant dominant signal component in the model proposed here to represent shadowed fading in D2D communications is considered as being Nakagami-m distributed due to its ability to approximate the lognormal distribution [22] and its mathematical tractability.

The complex received signal envelope $R\exp(j\theta)$ for this new model may be written as the sum of the resultant scattered waves (W) and the resultant dominant component (Δ) such that

$$R\exp(j\theta)=W\exp(j\phi)+\Delta\exp(j\phi_0) \tag{1}$$

where W, as shown in [16], follows a Nakagami-m distribution and Δ is also assumed to be Nakagami-m distributed. In this model, ϕ_0 is the phase of the resultant dominant component and ϕ is the stationary random phase process associated with W [23] distributed over the range $[-\pi,\pi)$. If Δ is initially held constant, then the conditional probability density function of R is given by

$$f_{R|\Delta}(r|\delta)=\frac{r^{\mu}}{\sigma^2\delta^{\mu-1}}\exp\left(-\frac{r^2+\delta^2}{2\sigma^2}\right)I_{\mu-1}\left(\frac{\delta r}{\sigma^2}\right) \tag{2}$$

which is that of the $\kappa-\mu$ distribution [16] parameterized in terms of δ, σ, and μ, and $I_{\nu}(\bullet)$ is the modified Bessel function of the first kind, order ν. Here κ is related to δ, σ, and μ through the relationship [16]

$$\kappa=\frac{\delta^2}{2\mu\sigma^2} \tag{3}$$

which is simply ratio of the total power of the dominant components (δ^2) to the total power of the scattered waves $(2\mu\sigma^2)$ where $\mu>0$ is related to the multipath clustering and the mean power is given by [16]

$$E[R^2]=\hat{r}^2=\delta^2+2\mu\sigma^2 \tag{4}$$

To determine the distribution of R when Δ varies according to the Nakagami-m distribution we now calculate the conditional mathematical expectation $\int_0^{\infty}f_{R|\Delta}(r|\delta)f_{\Delta}(\delta)d\delta$ which gives

$$f_R(r)=\frac{r^{\mu}}{\sigma^2}\int_0^{\infty}\frac{1}{\delta^{\mu-1}}\exp\left(-\frac{r^2+\delta^2}{2\sigma^2}\right)I_{\mu-1}\left(\frac{\delta r}{\sigma^2}\right)f_{\Delta}(\delta)d\delta \tag{5}$$

where

$$f_{\Delta}(\delta)=\frac{2m^m}{\Omega^m\Gamma(m)}\delta^{2m-1}\exp\left(\frac{-m\delta^2}{\Omega}\right) \tag{6}$$

In (6), $\Gamma(\bullet)$ is the gamma function and $m=E^2[\Delta^2]/\mathrm{var}[\Delta^2]$ is the Nakagami parameter where $\mathrm{var}[\Delta^2]$ is the variance [24]. In this instance, $\Omega=E[\Delta^2]$ is the average power of the resultant dominant component. In a similar fashion to [20], in the model proposed here, m is allowed to take any value in the range $m\geq 0$ where $m=0$ corresponds to complete shadowing of the resultant dominant component and $m\to\infty$ corresponds to no shadowing of the resultant dominant component. As noted in [20], the extreme cases of $m=0$ and $m=\infty$ cannot be met in reality. Using [25, p. 273, Equation 4], and after some mathematical manipulation, (5) can now be written as

$$f_R(r)=\frac{r^{2\mu-1}}{2^{\mu-1}\sigma^{2\mu}\Gamma(\mu)}\left(\frac{2m\sigma^2}{\Omega+2m\sigma^2}\right)^m\exp\left(-\frac{r^2}{2\sigma^2}\right)\times{}_1F_1\left(m;\mu;\frac{r^2\Omega}{2\sigma^2(\Omega+2m\sigma^2)}\right) \tag{7}$$

where ${}_1F_1(\bullet;\bullet;\bullet)$ is the confluent hypergeometric function [26]. Using equations (2) and (3) to perform a substitution of variables, it how becomes possible to express (7) in terms of κ, μ, $\hat{r}$, m and Ω as given in (8), shown at the bottom of the page.

$$f_R(r)=\frac{2r^{2\mu-1}}{\Gamma(\mu)}\left(\frac{\mu(1+\kappa)}{\hat{r}^2}\right)^{\mu}\left(\frac{m\hat{r}^2}{\mu(1+\kappa)\Omega+m\hat{r}^2}\right)^m\exp\left(-\frac{\mu(1+\kappa)r^2}{\hat{r}^2}\right){}_1F_1\left(m;\mu;\frac{\Omega\left(\mu(1+\kappa)r\right)^2}{\hat{r}^2\left(\mu(1+\kappa)\Omega+m\hat{r}^2\right)}\right) \tag{8}$$

$$E[R^n]=\frac{\Gamma\left(\mu+\frac{n}{2}\right)}{\Gamma(\mu)}\left(\frac{\hat{r}}{\sqrt{\mu(1+\kappa)}}\right)^n\left(\frac{m\hat{r}^2}{\mu(1+\kappa)\Omega+m\hat{r}^2}\right)^m{}_2F_1\left(m;\mu+\frac{n}{2};\frac{\mu(1+\kappa)\Omega}{\mu(1+\kappa)\Omega+m\hat{r}^2}\right) \tag{9}$$

$$f_S(s)=\frac{s^{\mu-1}}{\Gamma(\mu)}\left(\frac{\mu(1+\kappa)}{\hat{r}^2}\right)^{\mu}\left(\frac{m\hat{r}^2}{\mu(1+\kappa)\Omega+m\hat{r}^2}\right)^m\exp\left(-\frac{\mu(1+\kappa)s}{\hat{r}^2}\right){}_1F_1\left(m;\mu;\frac{s\Omega\left(\mu(1+\kappa)\right)^2}{\hat{r}^2\left(\mu(1+\kappa)\Omega+m\hat{r}^2\right)}\right) \tag{10}$$

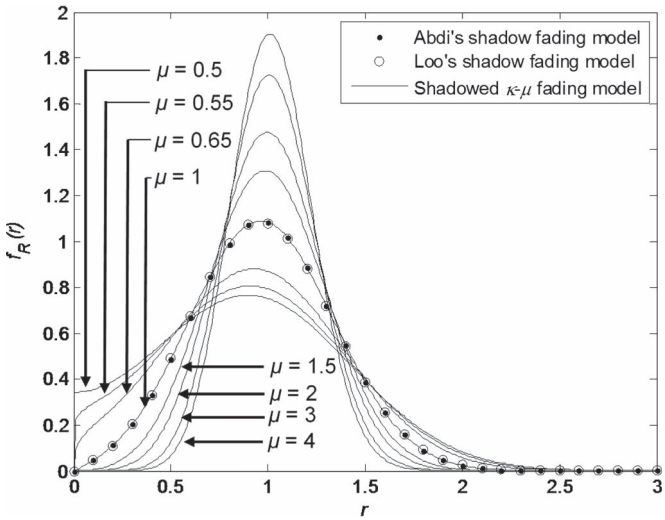

Fig. 2. Comparison of the PDFs for Abdi's shadowed fading model [20], Loo's shadowed fading model [21] and the shadowed $\kappa - \mu$ fading model for increasing μ. The values of α, β, m, Ω, and σ are the average values given in [20] while $\kappa = 2.968$, $\mu = 1$ and $\hat{r} = 1$.

The closed-form PDF in (8) is a new result, which models $\kappa - \mu$ fading in which the resultant dominant component is distributed according to the Nakagami-m PDF. It is a general model which will find application in other areas of communications such as land mobile satellite channels [20], [21]. Indeed Abdi's model, which assumes a shadowed Rice PDF, appears as a special case of (8) which is obtained by setting $\mu = 1$. Because of this relationship, (8) may also be used to approximate the model proposed in [21] which assumes that the LOS amplitude follows a lognormal distribution. Fig. 2 shows the PDF of the shadowed $\kappa - \mu$ fading model for increasing values of μ using the average parameter estimates for land mobile satellite channels given in [20, Table III]. Also shown for comparison are the PDFs for Abdi [20] and Loo's [21] models respectively. As we can see for the case when $\mu = 1$ (with $\kappa = 2.968$ and $\hat{r} = 1$), the new model proposed here matches Abdi's model exactly and gives an excellent approximation of Loo's model. Using [27, p. 822, Equation 4], the moments of the shadowed $\kappa - \mu$ fading PDF given in (8) can be expressed as (9), shown at the bottom of the previous page, where n represents the n^{th} moment of the distribution such that $n = 0, 1, 2, \ldots$ and ${}_2F_1(\bullet, \bullet; \bullet; \bullet)$ is the Gauss hypergeometric function [28], [29, Equation 15.1.1].

Letting $S = R^2$ represent the instantaneous power in the proposed model, the power probability density function can be written as (10), shown at the bottom of the previous page. A useful function related to (10) is the moment generating function which is defined as $M_S = E[\exp(-\eta S)]$. It plays an important role in the calculation of the bit error rate (BER) and symbol error rate (SER) of different modulation schemes over fading channels [20]. Letting $\rho = 1/\mu(1 + \kappa)$ and again using [27, p. 822, Equation 4] along with the relationship ${}_2F_1(a, b; b; z) = (1 - z)^{-a}$ [26, Equation 15.1.8], for $\eta \geq 0$ the MGF of the model proposed here can be derived as

$$M_S(\eta) = \frac{(\eta\rho\hat{r}^2 + 1)^{m-\mu}(m\rho\hat{r}^2)^m}{[(\eta\rho\hat{r}^2 + 1)(m\rho\hat{r}^2 + \Omega) - \Omega]^m} \qquad (11)$$

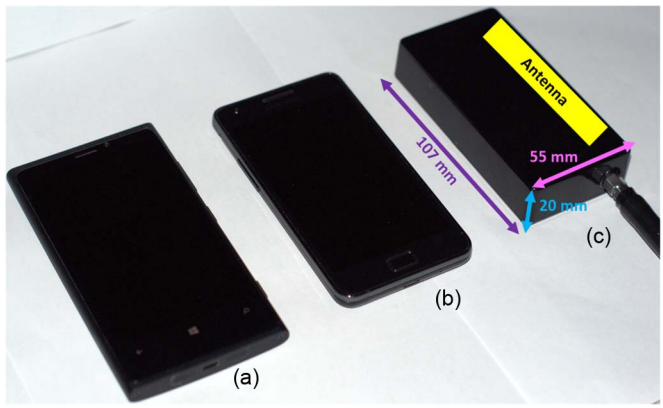

Fig. 3. Comparison of (a) Nokia 920, (b) Samsung Galaxy S2, and (c) the hypothetical UE used for the experimental part of the study.

IV. Measurement Setup

The device-to-device links considered in the experimental part of this study were formed using two Nearson S331AM-868 electrically short monopole antennas which were housed in a compact acrylonitrile butadiene styrene (ABS) enclosure. Fig. 3 shows the hypothetical UE alongside the popular Nokia 920 and Samsung Galaxy S2 handsets. As shown in Fig. 3, the setup was representative of the form factor of a smart phone which allowed the user to hold the device as they normally would to text, browse the net or make a voice call. It also allowed the user to carry the device in the pockets of their clothing. Each antenna was securely fixed to the inside of the enclosure in the position shown in Fig. 3(c) using a small strip of Velcro. The antennas were connected using low-loss coaxial cables to a Texas Instruments CC1110F32[2] system on chip which featured a CC1101 transceiver. The CC1110 was chosen for a number of reasons. Firstly, it operated within the European 868 MHz ISM band which is close to the 800 MHz LTE operating frequencies used in various parts of the Americas, Asia, Europe and Middle East and also the 850 band used in the US for GSM, IS-95 and 3G any of which could be used for future D2D communications. Secondly it offered straightforward programming of the radio registers and the ability to readily obtain the received signal strength which was critical for validating the use of the shadowed $\kappa - \mu$ fading model proposed in Section III for D2D channels.

For all of the measurements conducted in this study, unless otherwise stated, a device-to-device link was formed between two persons, namely person 1, a male of height 1.83 m and mass 94.7 Kg, and person 2, a female of height 1.57 m and mass 51.4 Kg. The hypothetical smart phone used by person 1 and herein denoted UE_1 was configured to operate at 868.3 MHz using a data rate of 500 kBaud with an output power of 0 dBm. It was programmed to continuously transmit packets with a period of 70 ms to UE_2 used by person 2. UE_2 was configured with a receive filter bandwidth of 812.5 kHz and set to record the packet reception time, sequence number and the received signal strength, which was stored for post-processing on a Dell XPS13 Ultrabook which featured an Intel i5-2467M processor, 4 GB of RAM and a 128 GB SSD. The receiver noise threshold

[2]http://www.ti.com/lit/ds/symlink/cc1110f32.pdf (05/14/2013)

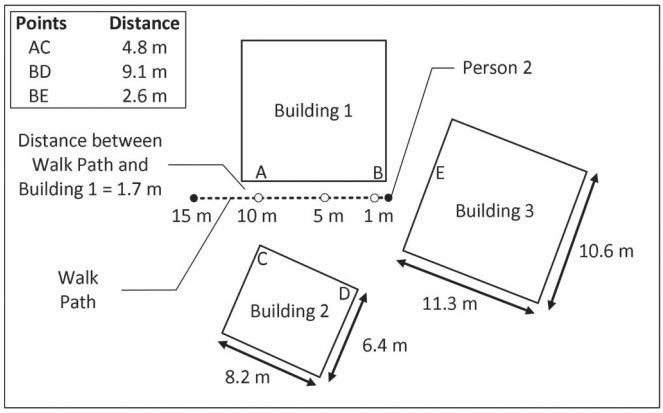

Fig. 4. Plan view of the measurement environment (not to scale) showing the measurement positions and walk path relative to the surrounding buildings. It should be noted that buildings 1 and 3 had the same structural dimensions.

was determined prior to all experiments and the average was found to be −103 dBm. Two primary[3] on-body positions for the UE were considered, namely the head and pocket. For all head measurements the UE was held at a 45 degree angle to the vertical against the respective person's right ear to imitate a voice call. The pocket location for person 1 was a front right trouser pocket, while for person 2 it was the front right pocket (at waist level) of a jacket. The elevation above ground level for each of the positions was as follows: UE_1 head, 1.65 m; UE_1 pocket, 0.80 m; UE_2 head, 1.42 m; UE_2 pocket, 0.85 m.

V. Channel Measurements and Modeling

The results presented in this Section were obtained from experiments performed in an outdoor urban environment. As shown in Fig. 4, the measurements were conducted in an open space between three buildings in a built up residential area in the suburbs of Belfast in the United Kingdom. Buildings 1 and 3 were two storey dwellings and had the same structural dimensions, while building 2 was a one storey structure. It should be noted that as well as the structural dimensions indicated in Fig. 4, buildings 1 and 3 had a height of 5.10 m from ground level to the lowest point of the roof level, while building 2 had a height of 2.40 m for the same dimension. The construction of all three buildings was typical of that encountered in the United Kingdom for these types of dwelling, with a brick and concrete block cavity wall structure, a number of double glazed exterior windows and a mixture of wooden and unplasticized polyvinyl chloride (uPVC) doors. In particular, building 1 featured 4 double glazed windows (spread over the ground and first floor levels) and a single uPVC door all situated on the wall adjacent to where the measurements were conducted (AB in Fig. 4). Building 2 had a single double glazed exterior window and a wooden door on the wall neighboring the measurement area (CD in Fig. 4), while building 3 featured two double glazed windows on the first floor level of the bounding wall. In the sequel, a number of different scenarios encompassing user rotation, random movements and mobility were considered. These activities were deemed representative of channel conditions likely to be encountered in everyday D2D links.

[3]A set of measurements in which UE_1 was held in the hand were also considered as discussed in Section V.

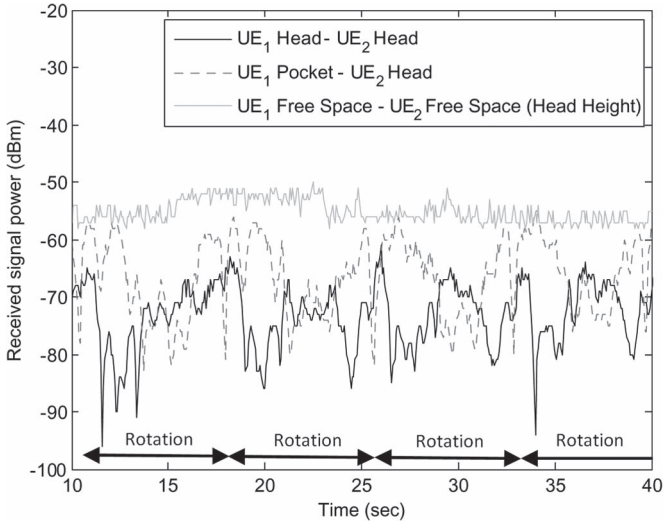

Fig. 5. Received signal power time series for UE_1 and UE_2 mounted on non-conductive stands and both the UE_1 head to UE_2 head channel and the UE_1 pocket to UE_2 head channel while person 1 performed repeated 360 degree rotations. Approximate rotation period denoted for the UE_1 head to UE_2 head channel.

A. Shadowed Fading Due to User Rotation and Random Movements

To assess the impact of user rotation in D2D links, UE_1 was initially held at person 1's head while they performed several repeated full 360 degree rotations directly in front of UE_2 at separation distances of 1 m, 5 m, 10 m, and 15 m (Fig. 4). Person 2 remained stationary for the duration of the measurements, facing in the direction of person 1, with UE_2 positioned at their head. This process was then repeated for UE_1 positioned in person 1's right trouser pocket and then again for UE_2 in person 2's front right jacket pocket. As a baseline, and to observe the potential impact of the human body in determining the received signal characteristics in D2D channels, Fig. 5 shows a 30 second segment of the received signal power time series when both UE_1 and UE_2 were positioned 5 m apart in free space using non-conductive stands. To allow a direct comparison with the UE_1 head to UE_2 head channel, the UEs were mounted on the stands using the same orientation i.e., at a 45 degree angle to the vertical with the same elevation from ground level. It should be noted that the very slight variation in the long-term mean signal level recorded for the baseline measurements was caused by local weather conditions on the day of measurements, which were windy.

Fig. 5 also shows the received signal power time series for the UE_1 head to UE_2 head channel when the user performed several repeated rotations at the same 5 m separation distance. The quasi-periodic variation of the received waveform caused by the movement (and associated shadowing) of the human body is clearly evident. What is more striking is that when the UEs were held in close proximity to the human body, peak-to-trough fade depths at this frequency can be as great as 30 dB. As shown in Fig. 5, this trend was also repeated when UE_1 was placed in person 1's trouser pocket. From these results alone, it is quite clear that human body shadowing will have a significant impact upon fading characteristics in D2D communications.

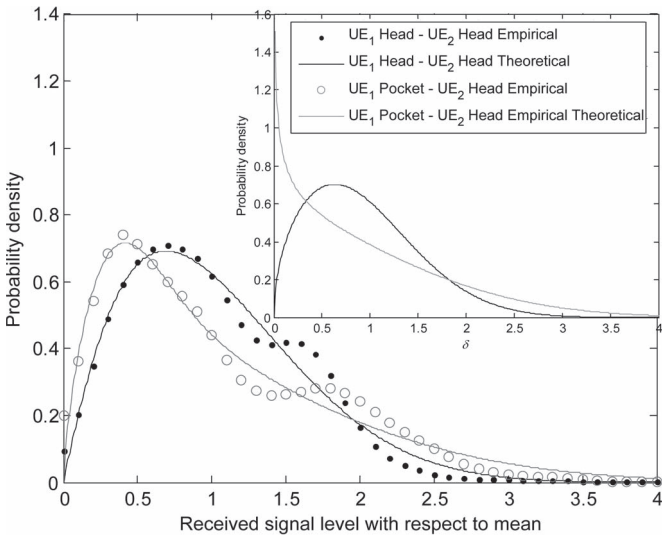

Fig. 6. Empirical and theoretical probability densities for UE_1 head to UE_2 head and UE_1 pocket to UE_2 head D2D channels. The estimated parameters for the UE_1 head to UE_2 head channel are $\hat{\kappa} = 8.49$, $\hat{\mu} = 0.96$, $\hat{r} = 1.44$, $\hat{m} = 0.74$, $\hat{\Omega} = 1.22$ and UE_1 pocket to UE_2 head channel $\hat{\kappa} = 3.80$, $\hat{\mu} = 0.84$, $\hat{r} = 1.01$, $\hat{m} = 0.38$, $\hat{\Omega} = 1.70$. Also shown inset is the distribution of the resultant dominant component.

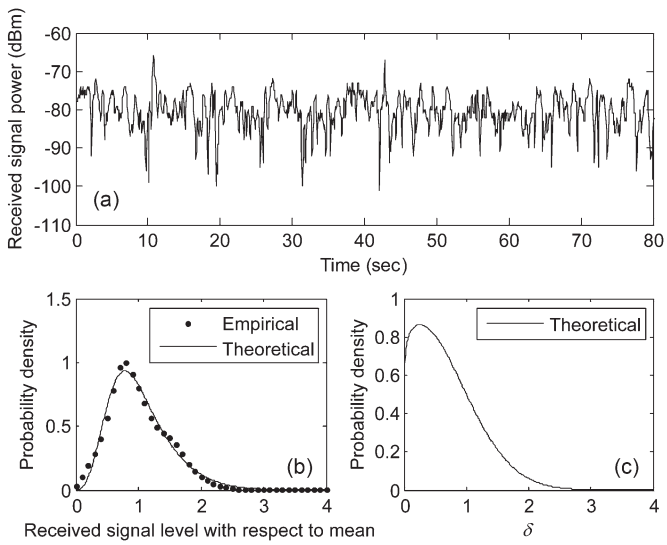

Fig. 7. (a) Received signal power time series (b) empirical and theoretical PDFs and (c) PDF of the resultant dominant component for the UE_1 head to UE_2 head channel while both persons performed random movements. The parameter estimates for the shadowed fading PDF are $\hat{\kappa} = 1.56$, $\hat{\mu} = 1.78$, $\hat{r} = 1.18$, $\hat{m} = 0.55$, and $\hat{\Omega} = 0.76$.

Fig. 6 shows the PDF of the shadowed $\kappa - \mu$ fading model fitted to the empirical PDF of the signal amplitude for the UE_1 head to UE_2 head and UE_1 pocket to UE_2 head channels while the user rotated at the 5 m separation distance. For convenience, the rms signal level, $\hat{r} = \sqrt{E[R^2]}$ is removed from the fading envelopes to enable a direct comparison of the fading characteristics for both links. All parameter estimates for the PDF of the shadowed $\kappa - \mu$ fading model were obtained using the `lsqnonlin` function available in the Optimization toolbox of MATLAB. As we can see, the PDF of the shadowed $\kappa - \mu$ fading model provides a good fit to the empirical PDF, particularly at low signal levels. It should be noted that a secondary mode was apparent in both empirical PDFs shown in Fig. 6. The origin of these artefacts may be explained as follows—to achieve a realistic characterization of shadow fading due to user rotation, the empirical PDF was constructed from a continuous data set in which the test subject performed a number of repeated rotations during a 60 second period. Considering the UE_1 head to UE_2 head (black trace) shown in Fig. 5, a clear pattern of signal variation from maxima (direct LOS) to minima (maximum shadowing) can be identified. However it can also be seen that due to slight differences in the test subject's gait while repeating the rotational movement, the received signal waveform varies between repetitions, in the process introducing different signal modes.

Also shown inset in Fig. 6 is the distribution of the resultant dominant component for each of the links plotted using equation (6). As we can see from Fig. 6, the characteristics of the shadowed fading of the resultant dominant component vary considerably, dependent upon whether UE_1 is positioned at the head or pocket. Although not shown due to space limitations, for the other rotational measurements (i.e., 1 m, 10 m, and 15 m), the estimated m parameter of the resultant dominant component was typically less than 0.5. This suggests that during user rotation, the resultant dominant component in outdoor D2D links will be subject to heavy shadowing.

For the random movements, person 1 stood at the 10 m position and person 2 took up their normal position as shown in Fig. 4. Both persons were initially stationary, in direct LOS and had the UEs positioned at their heads. They were then instructed to move around randomly within a circle of radius 1 m from their starting points while imitating a voice call. Fig. 7(a) shows the received signal power time series for the UE_1 head to UE_2 head channel while the users performed random movements. Due to the constantly changing orientation and posture of both persons, this channel was subject to considerable shadowed and multipath fading. This was confirmed by the parameter estimates for (8), here $\hat{\mu}$ and $\hat{m}$ were found to be 1.78 and 0.55 respectively which suggested both clustering of the multipath components and strong shadowing of the resultant dominant component. As we can see from Fig. 7(b), the PDF of the shadowed $\kappa - \mu$ fading model given in (8) provides an excellent fit to the measured data, while Fig. 7(c) shows the shadowing characteristics of the resultant dominant component.

B. Shadowed Fading Due to User Mobility

The next set of outdoor experiments were conducted along a 15 m straight line walk path, 1.7 m from the side of building 1 as shown in Fig. 4. For these measurements, the UEs were either positioned at the person's head or in their pocket as before. Person 2 again stood stationary, with their arms by their sides, facing in the direction of person 1. Person 1 then walked from the 15 m point to the point 1 m directly in front of person 2 before returning to the 15 m starting point. Prior to assessing the impact of UE mobility in D2D channels, the influence of the local environment upon the received signal characteristics was investigated. In a similar fashion to the baseline measurements detailed above, UE_1 and UE_2 were again mounted on

TABLE I
ESTIMATED PARAMETERS FOR ALL MOBILE D2D CHANNELS

Scenario	Shadowed Fading					Local Mean		Path Loss	
	$\hat{\kappa}$	$\hat{\mu}$	$\hat{r}$	$\hat{m}$	$\hat{\Omega}$	$\hat{\alpha}$	$\hat{\beta}$	$\hat{n}$	$\hat{P}_{dB}(d_0)$
Free Space									
UE_1 on trolley towards UE_2	481	0.01	0.98	2876	1.09	0.10	0.40	2.10	44.63
UE_2 at Head									
UE_1 at head walking towards UE_2	39.5	0.18	1.00	165	1.01	0.06	0.31	1.80	60.11
UE_1 at head walking away from UE_2	1.21	3.22	1.40	0.23	0.30	0.07	0.22	1.23	68.48
UE_1 in pocket walking towards UE_2	6.70	0.75	1.00	2.66	1.03	0.10	0.12	1.67	64.28
UE_1 in pocket walking away from UE_2	4.03	0.97	1.00	2.46	0.96	0.10	0.23	2.41	44.49
UE_1 browsing walking towards UE_2	1843	0.01	0.93	5.53	1.06	0.05	0.17	1.37	67.01
UE_1 browsing walking away from UE_2	14.5	0.45	1.00	5.27	1.01	0.08	0.39	2.35	53.11
UE_2 Front Jacket Pocket									
UE_1 at head walking towards UE_2	8.52	0.48	1.00	2268	0.96	0.08	0.37	1.56	62.14
UE_1 at head walking away from UE_2	1.08	3.13	1.42	1374	0.11	0.06	0.36	2.31	51.81
UE_1 in pocket walking towards UE_2	40.6	0.58	0.98	1.41	1.16	0.11	0.21	1.71	69.95
UE_1 in pocket walking away from UE_2	1.24	0.72	1.04	734	0.81	0.17	0.36	2.10	47.21
UE_1 browsing walking towards UE_2	48.1	0.78	1.00	2.20	0.98	0.13	0.24	1.70	67.63
UE_1 browsing walking away from UE_2	47.4	0.10	1.00	∞	1.04	0.09	0.23	1.87	56.38

*∞ relates to an estimated *m* value which is extremely large i.e. the resultant dominant component is deterministic

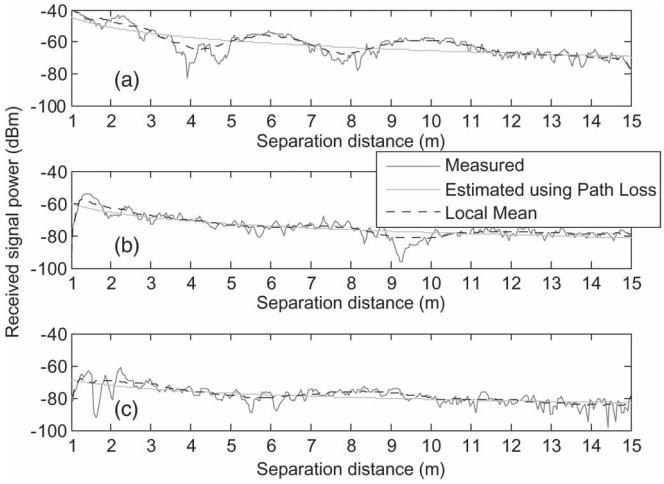

Fig. 8. Received signal power time series with received power level estimated using path loss and slow fading component for (a) UE_1 and UE_2 mounted on non-conductive stands and UE_1 head to UE_2 head while person was (b) walking towards person 2 and (c) walking away.

non-conductive stands with the hypothetical smart phones orientated to imitate being held at both users' head. The stand supporting UE_1 was then attached to a non-conductive trolley and moved along the walk path in the direction of UE_2.

Fig. 8(a) shows the measured received signal power time series for UE_1 and UE_2 oriented in the same configuration as a UE_1 head to UE_2 head channel however without the effect of the human body. As we can quite clearly see, when UE_1 was moved towards UE_2 there was a slow (or large-scale) fading component superimposed on the received signal by the local surroundings. Fig. 8(a) also shows the estimated received signal power which was determined from the measurements by converting the approximate velocity of the trolley to a distance and then fitting the log-distance path loss, $P_{dB} = P_{dB}(d_0) + 10n\log_{10}(d/d_0)$ to the data. Here, the path loss exponent is represented by n and the reference distance d_0 was taken to be 1 m. As shown in Table I, for this environment n was found to be 2.1 which is close to that for free space. The slow fading component, was then found by calculating the local mean over a distance of 5 wavelengths. Here, as elsewhere [30], the slow fading amplitude, X, is modeled as a lognormal process which is distributed according to

$$f_X(x) = \frac{1}{x\beta\sqrt{2\pi}} \exp\left[-\frac{(\ln x - \alpha)^2}{2\beta^2}\right] \tag{12}$$

where α and β are the location and scale parameters respectively. For all mobile measurements presented below, the same data treatment was applied. This process enabled the extraction of the shadowed fading which was due to the human body.

Figs. 8(b) and 8(c) show an example of the received signal power time series for the UE_1 head to UE_2 head channels as person 1 walked towards and then away from person 2 respectively. Also shown for comparison is the estimated received signal power based on the path loss and local mean signal level. The parameter estimates for n, $P_{dB}(d_0)$ and α and β are given in Table I. Fig. 9 shows the empirical and theoretical PDFs for the UE_1 head to UE_2 head channel as person 1 walked towards and then away from person 2. As we can see, the PDF of the shadowed $\kappa - \mu$ fading model given in (8) provides an excellent fit to the data proving the utility of the model for mobile D2D links. From Fig. 9 it is also evident that when person 1 walked in the direction of person 2, there was a strong resultant dominant component which was virtually unshadowed. However, when person 1 turned to walk

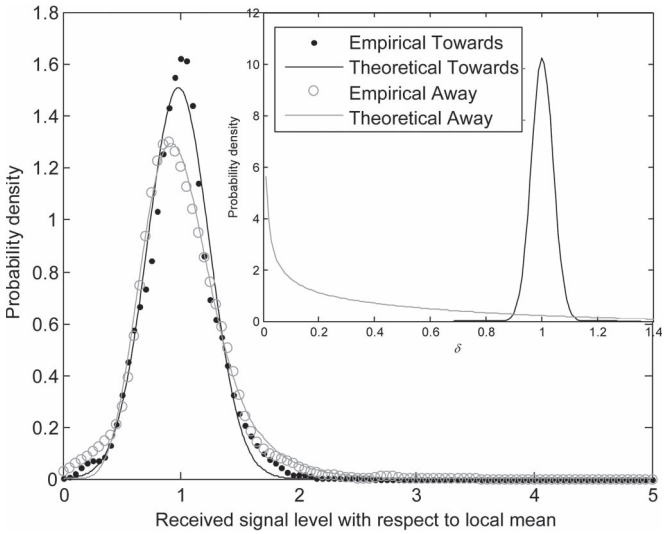

Fig. 9. Empirical and theoretical probability densities for UE_1 head to UE_2 head channel while person 1 was walking towards and away from person 2. Also shown inset is the distribution of the resultant dominant component. All parameter estimates are given in Table I.

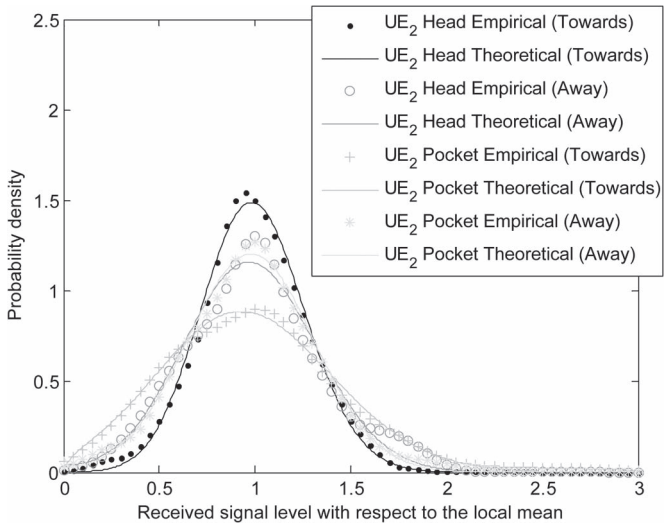

Fig. 10. Empirical and theoretical probability densities for all UE_1 browsing scenarios, all parameter estimates are given in Table I.

away from person 2 the dominant component became heavily shadowed and the signal received was primarily due to multipath propagation. As Table I shows, multipath clustering was evident for the UE_1 head to UE_2 head ($\hat{\mu} = 3.22$) and UE_1 head to UE_2 pocket ($\hat{\mu} = 3.13$) channels when person 1 walked away from person 2.

Another scenario which is likely to be encountered in D2D communications will occur when one person is browsing the web or "texting" using their smart device. To replicate this, person 1 was instructed to imitate browsing the web on their smart phone by holding UE_1 in their right hand (in front of their body), while at the same time walking along the trajectory shown in Fig. 4 towards and then away from person 2. For these measurements, UE_2 was once again positioned at either person 2's head or front right pocket. The parameter estimates for this scenario are provided in Table I. As we can see, quite strong dominant components were recorded for all of these channels possibly due to the geometry of the scenario in which UE_1 was held at a distance in front of person 1 meaning that UE_1 and UE_2 were always within LOS of each other. With the exception of the scenario in which person 1 emulated browsing the web while walking towards person 2 (UE_2 in person 2's pocket), the estimated m parameters for these channels were always greater than 5 suggesting that little variation of the resultant dominant component is experienced. The excellent fit of (8) to the fading characteristics observed in these channels is once again confirmed in Fig. 10.

VI. Conclusion and Future Work

A thorough knowledge of the D2D communications channel will be essential not only for the design of UE hardware, but also robust power control mechanisms and the optimization of protocols to be used in future D2D communications. This paper has focused on a small, but significant, part of this wide-ranging research problem by investigating the impact of human body shadowing in D2D links. To this end, a novel statistical model for shadowed fading in wireless communications channels has been proposed, namely the shadowed $\kappa - \mu$ fading model. In this new model the potential clustering of multipath components is considered alongside the presence of elective dominant signal components—a scenario which is similar to that observed in traditional $\kappa - \mu$ fading. One key difference between $\kappa - \mu$ fading and the model proposed here is that the resultant dominant component, formed by the phasor addition of the principal signal components, is subject to Nakagami-m fading. The PDF, moments and MGF of this model have been derived and are given in a convenient closed-form solution. The MGF in particular will be essential for calculating the BER and SER of different modulation schemes over shadowed fading channels. Although this new model was derived for the purpose of modeling shadowed fading in D2D communications, it will find application in many communications scenarios in which the received signal is subject to shadowed fading. For example, it will be immediately useful in the study of land mobile satellite communications and body centric communications where the main signal paths may also be subject to random shadowing.

The utility of the shadowed $\kappa - \mu$ fading model for outdoor D2D channels has been thoroughly validated through a series of experiments conducted for typical usage scenarios. It has been found that shadowing of the resultant dominant component can vary significantly depending upon the position of the user equipment relative to the body and the link geometry. For instance in D2D links in which one of the user's rotate, the dominant signal component can be heavily shadowed with the received signal power level varying by as much as 30 dB. In the majority of the D2D links studied here, when one UE is mobile, irrespective of whether the user is moving towards or away from the opposite end of the link, a dominant component can be observed in the statistics of the received signal. A range of the parameter estimates for the shadowed $\kappa - \mu$ fading model have been provided. These will be useful for those working on D2D communications as it will enable the simulation of the received signal for the testing of new D2D technologies.

As a final point, it is worth mentioning that while the characterization of shadowing in D2D channels is an important step towards a fuller understanding of this emerging type of wireless channel, there are many other open research questions relating to the D2D channel. One such issue is the prevalence of frequency selectivity which is known to occur in macro cellular environments. This knowledge will be vital for the successful implementation of technologies for multiuser D2D systems such as chunk-based resource allocation [31], which use orthogonal frequency division multiple access (OFDMA). Therefore a direct extension of the experimental work conducted in this study will be to investigate the correlation between neighboring frequencies used to support OFDMA for D2D communications.

ACKNOWLEDGMENT

The author would like to thank Mrs. Teresa Cotton and Ms. Lauryn Cotton for their assistance with the channel measurements conducted in this study.

REFERENCES

[1] C.-H. Yu, O. Tirkkonen, K. Doppler, and C. Ribeiro, "Power optimization of device-to-device communication underlaying cellular communication," in *Proc. IEEE Int. Conf. Commun.*, Jun. 2009, pp. 1–5.

[2] K. Doppler, M. Rinne, C. Wijting, C. B. Ribeiro, and K. Hugl, "Device-to-device communication as an underlay to LTE-advanced networks," *IEEE Commun. Mag.*, vol. 47, no. 12, pp. 42–49, Dec. 2009.

[3] L. Lei, Z. Zhong, C. Lin, and X. Shen, "Operator controlled device-to-device communications in LTE-advanced networks," *IEEE Wireless Commun.*, vol. 19, no. 3, pp. 96–104, Jun. 2012.

[4] M. J. Yang, S. Y. Lim, H. J. Park, and N. H. Park, "Solving the data overload: Device-to-device bearer control architecture for cellular data offloading," *IEEE Veh. Technol. Mag.*, vol. 8, no. 1, pp. 31–39, Mar. 2013.

[5] M. C. Erturk, S. Mukherjee, H. Ishii, and H. Arslan, "Distributions of transmit power and SINR in device-to-device networks," *IEEE Commun. Lett.*, vol. 17, no. 2, pp. 273–276, Feb. 2013.

[6] B. Kaufman, J. Lilleberg, and B. Aazhang, "Spectrum sharing scheme between cellular users and ad-hoc device-to-device users," *IEEE Trans. Wireless Commun.*, vol. 12, no. 3, pp. 1038–1049, Mar. 2013.

[7] H. Min, J. Lee, S. Park, and D. Hong, "Capacity enhancement using an interference limited area for device-to-device uplink underlaying cellular networks," *IEEE Trans. Wireless Commun.*, vol. 10, no. 12, pp. 3995–4000, Dec. 2011.

[8] G. Fodor *et al.*, "Design aspects of network assisted device-to-device communications," *IEEE Commun. Mag.*, vol. 50, no. 3, pp. 170–177, Mar. 2012.

[9] C. Xu *et al.*, "Interference-aware resource allocation for device-to-device communications as an underlay using sequential second price auction," in *Proc. IEEE Int. Conf. Commun.*, Jun. 2012, pp. 445–449.

[10] K. Doppler, M. P. Rinne, P. Janis, C. Ribeiro, and K. Hugl, "Device-to-device communications; functional prospects for LTE-advanced networks," in *Proc. IEEE Int. Conf. Commun. Workshops*, Jun. 2009, pp. 1–6.

[11] M. G. da S Rego, T. F. Maciel, H. de H M Barros, F. R. P. Cavalcanti, and G. Fodor, "Performance analysis of power control for device-to-device communication in cellular MIMO systems," in *Proc. Int. Symp. Wireless Commun. Syst.*, Aug. 2012, pp. 336–340.

[12] H. Xing and S. Hakola, "The investigation of power control schemes for a device-to-device communication integrated into OFDMA cellular system," in *Proc. IEEE Int. Symp. Pers., Indoor, Mobile Radio Commun.*, Sep. 2010, pp. 1775–1780.

[13] J. Gu, S. J. Bae, B.-G. Choi, and M. Y. Chung, "Dynamic power control mechanism for interference coordination of device-to-device communication in cellular networks," in *Proc. 3rd Int. Conf. Ubiquitous Future Netw.*, Jun. 2011, pp. 71–75.

[14] S. Obayashi and J. Zander, "A body-shadowing model for indoor radio communication environments," *IEEE Trans. Antennas Propag.*, vol. 46, no. 6, pp. 920–927, Jun. 1998.

[15] S. L. Cotton, A. McKernan, A. J. Ali, and W. G. Scanlon, "An experimental study on the impact of human body shadowing in off-body communications channels at 2.45 GHz," in *Proc. Eur. Conf. Antennas Propag.*, Apr. 2011, pp. 3133–3137.

[16] M. D. Yacoub, "The $\kappa - \mu$ distribution and the $\eta - \mu$ distribution," *IEEE Antennas Propag. Mag.*, vol. 49, no. 1, pp. 68–81, Feb. 2007.

[17] P. Van Torre *et al.*, "Characterization of measured indoor off-body MIMO channels with correlated fading, correlated shadowing and constant path loss," *IEEE Trans. Wireless Commun.*, vol. 11, no. 2, pp. 712–721, Feb. 2012.

[18] W. P. L. Cully, S. L. Cotton, W. G. Scanlon, and J. B. McQuiston, "Body shadowing mitigation using differentiated LOS/NLOS channel models for RSSI-based Monte Carlo personnel localization," in *Proc. IEEE Wireless Commun. Netw. Conf.*, Apr. 2012, pp. 694–698.

[19] S. L. Cotton and W. G. Scanlon, "An experimental investigation into the influence of user state and environment on fading characteristics in wireless body area networks at 2.45 GHz," *IEEE Trans. Wireless Commun.*, vol. 8, no. 1, pp. 6–12, Jan. 2009.

[20] A. Abdi, W. C. Lau, M.-S. Alouini, and M. Kaveh, "A new simple model for land mobile satellite channels: First- and second-order statistics," *IEEE Trans. Wireless Commun.*, vol. 2, no. 3, pp. 519–528, May 2003.

[21] C. Loo, "A statistical model for a land mobile satellite link," *IEEE Trans. Veh. Technol.*, vol. VT-34, no. 3, pp. 122–127, Aug. 1985.

[22] S. L. Cotton and W. G. Scanlon, "Higher order statistics for lognormal small-scale fading in mobile radio channels," *IEEE Antennas Wireless Propag. Lett.*, vol. 6, pp. 540–543, 2007.

[23] I. B. G. Porto, M. D. Yacoub, J. C. S. Santos Filho, S. L. Cotton, and W. G. Scanlon, "Nakagami-m phase model: Further results and validation," *IEEE Wireless Commun. Lett.*, vol. 2, no. 5, pp. 523–526, Oct. 2013.

[24] M. D. Yacoub, J. E. V. Bautista, and L. Guerra de Rezende Guedes, "On higher order statistics of the Nakagami-m distribution," *IEEE Trans. Veh. Technol.*, vol. 48, no. 3, pp. 790–794, May 1999.

[25] A. P. Prudnikov, Y. A. Brychkov, and O. I. Marichev, *Integrals and Series, Vol. 2: Special Functions*. Moscow, Russia: Fiziko-Matematicheskaya Literatura, 2003.

[26] J. Abad and J. Sesma, "Computation of the regular confluent hypergeometric function," *Math. J.*, vol. 5, no. 4, pp. 74–76, 1995.

[27] I. S. Gradshteyn, I. M. Ryzhik, A. Jeffrey, and D. Zwillinger, *Table of Integrals, Series, Products*, 7th ed. London, U.K.: Academic, 2007.

[28] W. Magnus, F. Oberhettinger, and R. P. Soni, *Formulas and Theorems for the Special Functions of Mathematical Physics*, 3rd ed. New York, NY, USA: Springer-Verlag, 1966.

[29] M. Abramnowitz and I. A. Stegun, *Handbook of Mathematical Functions*. Washington, DC, USA: U.S. Dept. of Commerce, National Bureau of Standards, 1972.

[30] M. Pätzold and V. D. Nguyen, "A spatial simulation model for shadow fading processes in mobile radio channels," in *Proc. IEEE Int. Symp. Pers., Indoor, Mobile Radio Commun.*, Sep. 2004, vol. 3, pp. 1832–1838.

[31] H. Zhu and J. Wang, "Chunk-based resource allocation in OFDMA systems—Part I: Chunk allocation," *IEEE Trans. Commun.*, vol. 57, no. 9, pp. 2734–2744, Sep. 2009.

Simon L. Cotton (S'04–M'07–SM'14) received the B.Eng. degree in electronics and software from the University of Ulster, Ulster, U.K., in 2004 and the Ph.D. degree in electrical and electronic engineering from Queen's University of Belfast, Belfast, U.K., in 2007.

He is currently a Lecturer in wireless communications and an EPSRC/Royal Academy of Engineering Research Fellow with the Institute of Electronics, Communications and Information Technology (ECIT), Queen's University Belfast. He is also a Co-founder of and the Chief Technology Officer with ActivWireless Ltd, Belfast, U.K. He has authored and coauthored over 80 publications in major IEEE/IET journals and refereed international conferences, two book chapters, and two patents. Among his research interests are cellular device-to-device, vehicular, and body-centric communications. His other research interests include radio channel characterization and modeling and the simulation of wireless channels.

Dr. Cotton was awarded the H. A. Wheeler Prize, in July 2010, by the IEEE Antennas and Propagation Society for the best applications journal paper in the IEEE TRANSACTIONS ON ANTENNAS AND PROPAGATION during 2009. In July 2011, he was awarded the Sir George Macfarlane Award from the U.K. Royal Academy of Engineering in recognition of his technical and scientific attainment since graduating from his first degree in engineering.